ELSEVIER

Journal of Alloys and Compounds 434–435 (2007) 760–763

Journal of ALLOYS AND COMPOUNDS

www.elsevier.com/locate/jallcom

Electrochemical hydrogen insertion in Mg–La(Mm)Ni_5 nanocomposites

A. Borissova[a], S. Bliznakov[b], T. Spassov[a,*]

[a] Department of Chemistry, University of Sofia "St. Kl. Ohridski", 1 J. Bourchier Str., 1126 Sofia, Bulgaria
[b] Institute of Electrochemistry and Energy Systems, Bulgarian Academy of Sciences, Acad. G. Bonchev Str., bl. 10, 1113 Sofia, Bulgaria

Abstract

The electrochemical hydriding/dehydriding of a series of Mg–x at.% Mm(La)Ni_5 (Mm = La-rich mischmetal) nanocomposites was investigated. The composites were produced by mechanical milling in a planetary mill under Ar atmosphere. The starting materials were MgH_2 and $MmNi_5$ or $LaNi_5$. For all compositions, except Mg–5 at.% $MmNi_5$, during the first 1–2 h of milling under argon, MgH_2 decomposes completely and during the following milling, formation of new compounds (mainly Mg_2Ni) takes place. Very fast gas phase hydrogen absorption/desorption kinetics was determined for all composites. Significant difference in the electrochemical properties (discharge capacity and cycle life) is found between the composites with $LaNi_5$ and these with $MmNi_5$ as well as between the composites with different $MmNi_5$ content. The discharge capacities calculated are between 30 and 115 mAh g^{-1}. Reducing the corrosion of the composites by minimizing its contact with the electrolyte results in substantially higher and stable with cycling capacity (360 mAh g^{-1} for Mg–10 at.% $MmNi_5$).

Keywords: Nanostructured materials; Mg composites; Mechanical alloying; Electrochemical insertion

1. Introduction

NiMH batteries development appears to be a solution for the replacement of NiCd-type batteries due to their environment compatibility combined with high specific energy. The progress in this direction requires extensive investigation of new materials, which can be used for negative electrodes. The most studied AB_5 ($LaNi_5$, $MmNi_5$) and AB_2 ($ZrNi_2$ and ZrV_2) type alloys were substantially improved and already in use. Nevertheless, the capacity of these materials is relatively low and their activation is slow [1,2]. Recently, investigations were focussed on Mg–Ni systems [3–8] with poor hydrogen absorption/desorption kinetics and bad corrosion resistance in alkaline solution. These materials reveal a high theoretical capacity and lack of activation period, but formation of $Mg(OH)_2$ impedes the extraction of maximum capacity and limits their application. In order to combine the properties of both systems (Mg–Ni and La–Ni), new ternary alloys with general formula $REMg_2Ni_9$ (RE: rare earth, Ca, Y) were investigated [9–11]. After the discovering that RE–Mg–Ni based alloy with $PuNi_3$ hexagonal structure can absorb and desorb reversibly 1.8–1.87 wt.% H_2 [12,13] studies for improving their electrochemical properties by different additions have started. Chen et al. reported a discharge capacity of 356 mAh g^{-1} for $LaCaMgNi_9$ [14]. Kohno et al. reported discharge capacity of 410 mAh g^{-1} for $La_{0.7}Mg_{0.3}Ni_{2.8}Co_{0.5}$ [15] and good cycling stability within 30 cycles. Similar results were obtained by Liao et al. [16] for La_2MgNi_9—capacity of 400 mAh g^{-1}. Therefore, RE–Mg–Ni–based alloys appear to be a good potential candidates for the negative electrode in Ni–MH battery. It is also reported that $LaMg_2Ni_9$ ($PuNi_3$-structure) has low hydrogen capacity (about 0.33 wt.%), but when La and Mg were partially replaced by Ca the capacity of $(La_{0.65}Ca_{0.35})(Mg_{1.32}Ca_{0.68})Ni_9$ [12] rises to 1.87 wt.% together with increasing the cell volume. Zhang et al. [17] studied the influence of rare earth elements on the structure and electrochemical properties of $RENi_3$ alloys (RE: La, Ce, Pr, Nd, Sm, Gd,) and found that YNi_3 shows satisfactory electrochemical characteristics, discharge capacity and discharge rate.

In our recent study [18] low temperature hydriding from a hydrogen gas phase was found for ball-milled Mg–10 at.% $MmNi_5$ nanocomposite and the hydrogen capacity was relatively high, ~3.5 wt.% H_2. Therefore, in our present work Mg–Mm(La)Ni_5 nanocomposites with different compositions were produced by high energy ball milling (BM) and their electrochemical hydriding/dehydriding was studied.

---

* Corresponding author. Tel.: +359 2 816 1236; fax: +359 2 9625438.
E-mail addresses: aborissova@chem.uni-sofia.bg (A. Borissova), sbliznakov@mail.bg (S. Bliznakov), tspassov@chem.uni-sofia.bg (T. Spassov).

0925-8388/$ – see front matter © 2006 Elsevier B.V. All rights reserved.
doi:10.1016/j.jallcom.2006.08.158

2. Experimental

Mg–*x* at.% Mm(La)Ni_5 composites were prepared from MgH_2 and $MmNi_5$ as starting materials, where Mm is mischmetal with a composition of about 50 at.% La, 30 at.% Ce and 20 at.% Nd, Pr, etc. The synthesis was carried out in a planetary milling device under 5 bar of Ar and balls to powder mass ratio 1:6. The duration of milling was 10 h. X-ray diffraction measurements were carried out with TUR-62 which using Cu Kα (λ = 1.54178 Å) radiation. The morphology of the as-milled composites was studied by scanning electron microscopy, JEOL model JSM-5510. Gas phase hydrogenation and dehydrogenation (PCT measurements) were preformed by Sievert's apparatus at 300 °C.

The electrochemical properties of the nanocomposites were investigated in a three-electrode cell. Nickel mesh was used as a counter (positive) electrode, Hg/HgO as a reference electrode and the studied materials as a working (negative) electrode. Six molars of KOH was used as electrolyte. Electrochemical hydrogen charge and discharge cycling tests were realised using potentiostat/galvanostat operating in a galvanostatic mode. Two prescriptions were used for the electrode preparation. One consists of mixing the as-milled powder with carbon black in proportion 1:4; water solution of PVA (polyvinyl alcohol) is added to moisten the so-prepared mixture. The homogenized blend was pressed with pressure of 150 kg cm^{-2} to form a tablet. The regime of charging in this case was C/30, i.e. insertion of 1/30 part of the maximum theoretical capacity within 1h. The discharge was carried out with 40 mA g^{-1} and with 60 mA g^{-1} (for the alloys after hydrogen gas phase activation) to 600 mV cut off potential with respect to Hg/HgO.

The second procedure for electrode preparation, includes homogenization of a mixture from the alloy powders and 25 wt.% teflonized carbon black (Vulcan 72®) in weight ratio 1:1 and pressing in 1 cm^2 matrix at pressure of 200 kg cm^{-2}. The charging was with 100 mA g^{-1} for 3 h in order to observe the difference in the values of the discharge capacity in a faster regime. The discharge was performed with 50 mA g^{-1} to −500 mV cut off potential (versus Hg/HgO).

In order to improve the corrosion stability of the electrodes prepared from the Mg–AB_5 nanocomposites in alkaline electrolytes a two-layer electrode technique was applied. A homogenized mixture of $MmNi_5$ and teflonized carbon black in weight ratio 1:1 was fixed in the matrix on both sides of a tablet, prepared from Mg–Mm(La)Ni_5 nanocomposite, at pressure of 100 kg cm^{-2}. The as prepared two-layer (sandwich-like) structure was pressed at 200 kg cm^{-2}. This electrode preparation technique combines the properties of the gas-diffusion electrodes to avoid the electrolyte penetration into the bulk of the electrode and the ability for reversible electrochemical hydriding of Mg–AB_5 composites containing a component (e.g. Mg, Mg_2Ni phases) with higher capacity and low corrosion stability in alkaline electrolytes.

3. Results and discussion

X-ray diffraction patterns of the as-milled Mg–5 at.% $MmNi_5$ and Mg–15 at.% $MmNi_5$ powders are presented in Fig. 1. Hexagonal $LaNi_5$ phase, used as a starting material, is clearly observed. The diffraction peaks of $LaNi_5$ are shifted to smaller angles. The peaks displacement, associated with an increase of the lattice parameters, is smaller for Mg–5% AB_5 compared to Mg–15% AB_5 nanocomposite. On the other hand, part of the nickel coming from $MmNi_5$ reacts with Mg to form Mg_2Ni, which is observed by XRD for both composites. Diffraction peaks of MgH_2 are found only in the XRD pattern of Mg–5% $MmNi_5$. Possible reason for the incomplete decomposition of MgH_2 is the smaller quantity of $MmNi_5$, probably acting as a catalyst, which is not sufficient to decompose completely the starting MgH_2 during the milling process. Pure Mg was not detected in both as-milled samples due to its participation in the formation of Mg_2Ni. Small amount of disordered (amorphous) phase with Mg participation is also possible to be formed during the milling process. The average size of the crystallites, calculated by the Scherrer equation, is about 30 nm for both main phases Mg_2Ni and $LaNi_5$ in the as-milled composites.

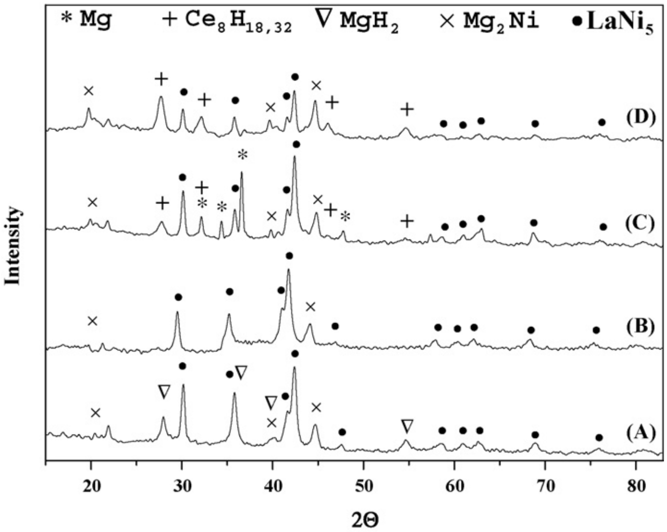

Fig. 1. X-ray diffraction patterns of: (A) as-milled Mg–5 at.% $MmNi_5$, (B) as-milled Mg–15 at.% $MmNi_5$, (C) Mg–5 at.% $MmNi_5$, after hydrogen desorption, and (D) Mg–15 at.% $MmNi_5$, after hydrogen desorption.

The morphology of the as-milled nanocomposites as well as the particle size distribution have been studied by SEM, Fig. 2. For both composites the size of the particles varies from 0.1 to about 10 μm with an average of about 5–6 μm, as the particles shape is uniform and oval. The larger particles are actually agglomerates of much smaller ones (<1 μm).

Hydrogen absorption and desorption kinetic curves at 300 °C are shown in Fig. 3. After short activation (one cycle only) both absorption and desorption processes proceed with a very high velocity, substantially higher than that of nanocrystalline Mg [19]. Comparing the kinetics of the two composites it can be seen that the hydriding of Mg–15 at.% $MmNi_5$ is significantly faster, especially in the final part of the process, than that of Mg–5 at.% $MmNi_5$.

The microstructure of the nanocrystalline powders was studied after the fourth cycle of gas phase hydrogen absorption/desorption at 300 °C (Fig. 1). $LaNi_5$ phase stays stable during hydriding/dehydriding at 300 °C, although its amount decreases after cycling. Mg_2Ni is found in both samples, as its amount slightly increases with cycling. Pure Mg is detected only in the sample with less $MmNi_5$. The average crystal size of all phases present increases insignificantly as a result of the heat treatment to about 40–45 nm. Small amount of CeH_x forms during cycling as well and appears to be stable during heating up to 300 °C. These results are in good agreement with those obtained recently by Delchev et al. [18].

A comparison between the maximum electrochemical discharge capacity of the Mg–5 at.% $MmNi_5$ and Mg–15 at.% $MmNi_5$ nanocomposites is presented in Figs. 4 and 5. To study the influence of the phase composition on the electrochemical hydrogenation, electrodes from Mg–10 at.% $MmNi_5$ and Mg–10 at.% $LaNi_5$ were measured as well. Maximum discharge capacity of 115 mAh g^{-1} was measured for Mg–15 wt.%

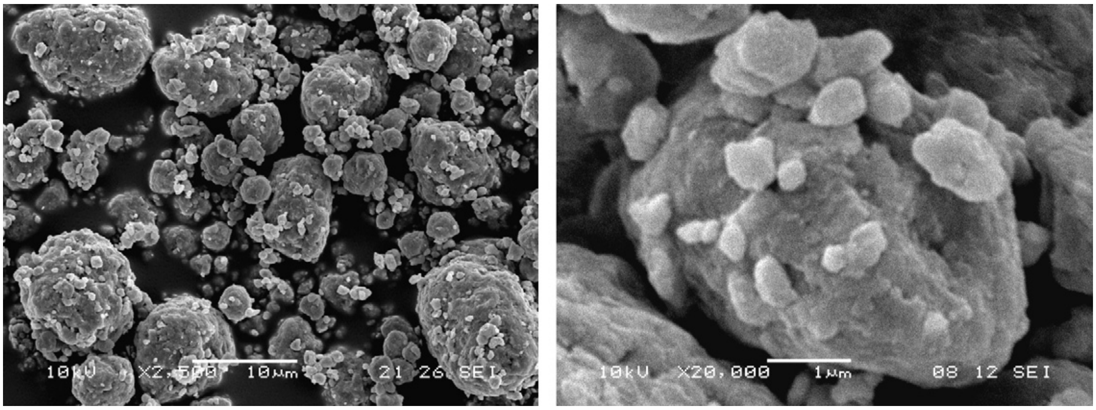

Fig. 2. SEM micrographs of as-milled Mg–15 at.% $MmNi_5$.

$MmNi_5$, which decays with cycling reaching 75 mAh g^{-1} at the fifth cycle. The highest measured value of the effective capacity corresponds to hydrogen content of 0.5 wt.%. The composite with 10 at.% $MmNi_5$ starts with a capacity of 60–65 mAh g^{-1}, which decreases to 30 mAh g^{-1} for seven cycles. The initial capacity of the composite with 5 at.% $MmNi_5$ is the lowest (∼40 mAh g^{-1}), but it shows a very slow improvement with cycling. Generally, the capacity and cycle life of all Mg-based composites studied are low and show typical for Mg–Ni based alloys values [3–8]. The most probable reason for these unsatisfactory electrochemical characteristics is the formation of $Mg(OH)_2$ on the electrode surface, leading to passivation of the particles surface.

A potential plateau of about −880 mV was observed for the composites with 10 and 15 at.% $MmNi_5$, which is typical for the $MmNi_5$-type alloys. The electrode prepared from Mg–5 at.% $MmNi_5$ practically does not reveal a plateau and the measured capacity is very low. The plateau of the Mg composite containing 10 at.% $LaNi_5$ is higher with about 30 mV and corresponds to that of $LaNi_5$-type alloys.

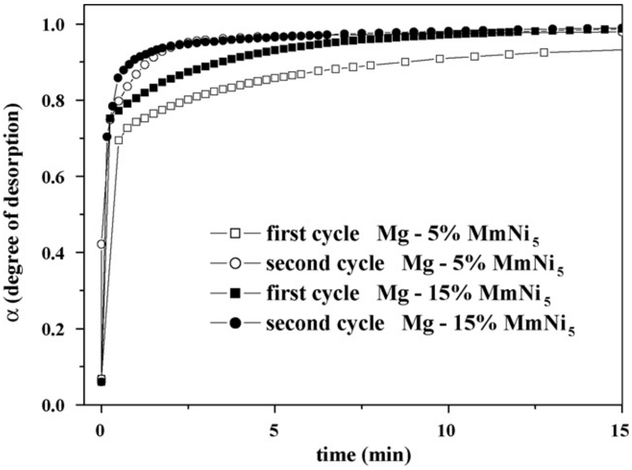

Fig. 3. Degree of hydrogen desorption vs. time, $\alpha(t)$, curves for Mg–5 at.% $MmNi_5$ and Mg–15 at.% $MmNi_5$.

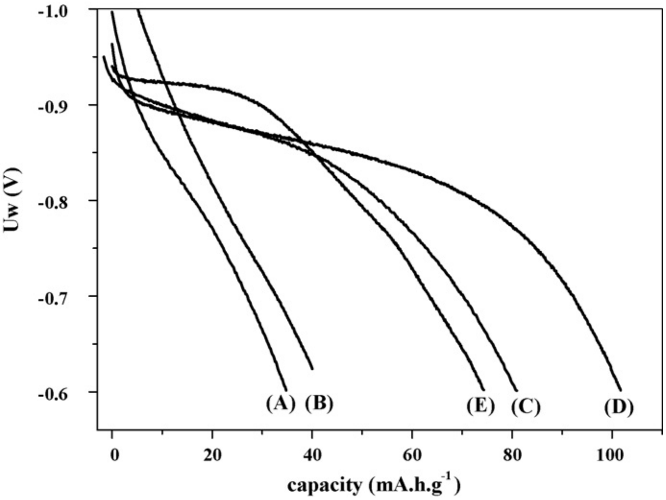

Fig. 4. Electrochemical discharge curves (Uw(V), potential of working electrode, measured vs. Hg/HgO) of: (A) Mg–5 at.% $MmNi_5$ after solid–gas desorption, (B) as-milled Mg–5 at.% $MmNi_5$, (C) Mg–15 at.% $MmNi_5$ after desorption, (D) as-milled Mg–15 at.% $MmNi_5$, and (E) Mg–10 at.% $LaNi_5$.

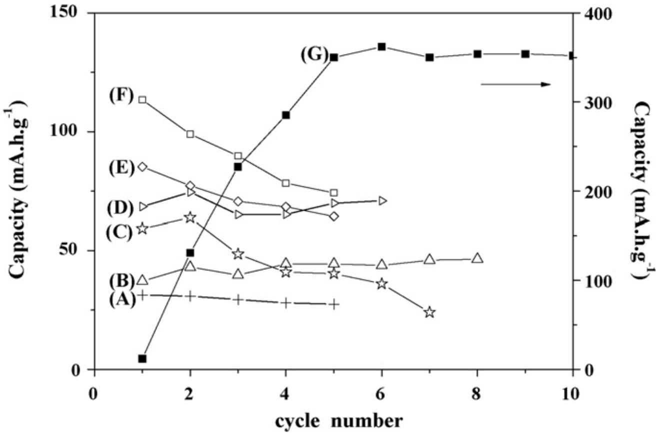

Fig. 5. Discharge capacity vs. cycle number of: (A) Mg–5 at.% $MmNi_5$ after H-desorption, (B) as-milled Mg–5 at.% $MmNi_5$, (C) as-milled Mg–10 at.% $MmNi_5$, (D) as-milled Mg–10 at.% $LaNi_5$, (E) Mg–15 at.% $MmNi_5$ after desorption, (F) as-milled Mg–15 at.% $MmNi_5$, and (G) “two-layer” electrode, prepared from Mg–10 at.% $MmNi_5$.

Electrodes, prepared from the composites after gas phase hydriding/dehydriding cycling at 300 °C were also investigated in order to study the effect of the microstructure change and preliminary activation in a hydrogen gas phase on the electrochemical performance of the composites. The measured value of the capacity was lower compared to that of the as-milled samples, which can be explained by the coarsening of the microstructure, proved by XRD.

From the results thus obtained it is important to mention that the electrochemical capacity measured, although being low, cannot be explained by the amount of the $MmNi_5$ (or $LaNi_5$) phase present in the composites only. The contribution of the Mg_2Ni phase to the overall capacity is clearly detected, although due to its fast corrosion the cycling behaviour is bad. Important proof of this result is the electrochemical charge/discharge of an electrode, prepared with the composite Mg–10 at.% $MmNi_5$, using a technique described in the experimental part, allowing to avoid the contact between the KOH electrolyte and the composite. The capacity obtained with the two-layer electrode ($360\,\mathrm{mAh\,g^{-1}}$) is with about $70\,\mathrm{mAh\,g^{-1}}$ higher than that measured with an electrode prepared from $MmNi_5$ only.

4. Conclusions

A series of Mg–Mm(La)Ni_5 nanocomposites have been prepared by ball milling and microstructurally characterized by SEM and XRD. Their electrochemical hydrogen charge/discharge behaviour was studied in galvanostatic conditions.

The milling was performed under Ar with MgH_2 and $MmNi_5$ or $LaNi_5$ as starting materials. As a result of the milling new phases (mostly Mg_2Ni) were formed. After gas phase hydrogenation/dehydrogenation cycling the nanocomposites contained $LaNi_5$, Mg_2Ni and CeH_x; pure Mg was detected only in Mg–5% $MmNi_5$. The grain size of the as-milled materials (∼30 nm) does not change significantly during hydrogen absorption/desorption cycling.

For all the compositions studied, low discharge capacities were measured due to the fast corrosion and formation of $Mg(OH)_2$ in alkaline solution. Relatively high and stable with cycling electrochemical capacity ($360\,\mathrm{mAh\,g^{-1}}$) was obtained for Mg–10 at.% $MmNi_5$ only when the corrosion was strongly reduced by avoiding contact between the negative electrode and KOH electrolyte. Further, investigation of the electrochemical charge/discharge behaviour of Mg–AB_5 nanocomposites with different compositions is underway.

Acknowledgments

The work is realised by financial support of EU project for Research and Training Network HPRN-CT-2002-00208 and partially supported by the Bulgarian Scientific Research Fund under grant BYX-14/05. The authors thank P. Delchev and Ts. Himitlijska for the help in the gas-phase experiment performance and N. Dimitrov for technical assistance in the SEM experiments.

References

[1] T. Sakai, I. Uehara, H. Ishikawa, M. Matsuoka, C. Iwakura, J. Alloys Compd. 293–295 (1999) 762–769.
[2] D.M. Kim, K.J. Jang, J.Y. Lee, J. Alloys Compd. 293–295 (1999) 583–592.
[3] H. Niu, D.O. Northwood, Int. J. Hydrogen Energy 27 (2002) 69–77.
[4] N. Cui, J.L. Luo, K.T. Chuang, J. Alloys Compd. 302 (2000) 218–226.
[5] H.Y. Lee, N.H. Goo, W.T. Jeong, K.S. Lee, J. Alloys Compd. 313 (2000) 258–262.
[6] S.I. Yamamura, H.Y. Kim, H. Kimura, A. Inoue, Y. Arata, J. Alloys Compd. 339 (2002) 230–235.
[7] H. Yuan, Q. Li, H. Song, Y. Wang, J. Liu, J. Alloys Compd. 353 (2003) 322–326.
[8] S. Nohara, N. Fujita, S.G. Zhang, H. Inoue, C. Iwakura, J. Alloys Compd. 267 (1998) 76–78.
[9] K. Kadir, T. Sakai, I. Uehara, J. Alloys Compd. 257 (1997) 115–121.
[10] K. Kadir, N. Nuriyama, T. Sakai, I. Uehara, L. Eriksson, J. Alloys Compd. 284 (1999) 145–154.
[11] K. Kadir, T. Sakai, I. Uehara, J. Alloys Compd. 287 (1999) 264–270.
[12] K. Kadir, T. Sakai, I. Uehara, J. Alloys Compd. 302 (2000) 112–117.
[13] J. Chen, H.T. Takeshita, H. Tanaka, N. Kuriyama, T. Sakai, J. Alloys Compd. 302 (2000) 304–313.
[14] J. Chen, N. Kuriyama, H.T. Takeshita, H. Tanaka, T. Sakai, M. Haruta, Electrochem. Solid State Lett. 3 (6) (2000) 249–252.
[15] T. Kohno, H. Yoshida, F. Kawashima, T. Inaba, I. Sakai, M. Yamamoto, M. Kanda, J. Alloys Compd. 311 (2000) L5–L7.
[16] B. Liao, Y.Q. Lei, G.L. Lu, L.X. Chen, H.G. Pan, Q.D. Wang, J. Alloys Compd. 356/357 (2003) 746–749.
[17] X. Zhang, W. Yin, Y. Chai, M. Zhao, Mater. Sci. Eng. B 117 (2005) 123–128.
[18] P. Delchev, Ts. Himitlijska, T. Spassov, J. Alloys Compd. 417 (2006) 85–91.
[19] W. Oelerich, T. Klassen, R. Borman, J. Alloys Compd. 315 (2001) 237–242.